Asian Journal of Chemistry; Vol. 26, No. 20 (2014), 6783-6786

ASIAN JOURNAL OF CHEMISTRY

http://dx.doi.org/10.14233/ajchem.2014.16767

Structure and Magnetic Properties of Yttrium-Doped M-Type Strontium Ferrite

XIAO-FEI NIU[1,2] and MING-YU ZHANG[1,*]

[1]Anhui Key Laboratory of Spintronics and Nanomaterials Research,Suzhou University, Suzhou 234000, P.R. China
[2]School of Physics and Material Science of Anhui University, Hefei 230039, P.R. China

*Corresponding author: E-mail: 65666409@qq.com

Received: 27 November 2013; *Accepted*: 13 March 2014; *Published online*: 25 September 2014; AJC-16009

In this paper we have prepared yttrium-doped M-type strontium ferrite $SrY_xFe_{(12-x)}O_{19}$ (x = 0, 0.25, 0.5, 0.75, 1) calcined materials by solid-phase sintering method at 1150 °C for 3 h. Then the calcined materials were pressed for magnets under the condition of oriented magnetic field and sintered in 1295 °C for 3 h. We have used X-ray diffraction, scanning electron microscope and magnetic tester analyze the phase structure of the sintered magnets, the surface morphology of the sintered magnet and the magnetic properties of the sintered magnets, respectively. The results showed that with the increase of yttrium-doped, the lattice constant 'a' increases first of all and then decreases 'c' increases slowly, a/c first increases and then decreases, crystal X-ray density $d_{x\text{-}ray}$ approximation increases linearly. SEM showed that the magnet has prepared a typical hexagonal structure morphology. Magnetic studies showed that with the doping of yttrium increase, the remanence B_r increasing monotonically, intrinsic coercivity H_{cj} and maximum energy product $(BH)_{max}$ and coercivity magnetic induction H_{cb} are first increases and then decreases. When the x = 1, have the maximum remanence B_r with 420.7 mT, but the intrinsic coercivity H_{cj} decreases to a minimum value; when x = 0.75 the intrinsic coercivity H_{cj} have a maximum value of 323.7 KA·m^{-1} and the remanence B_r reach 410.4 mT.

Keywords: Yttrium-doped, $SrY_xFe_{(12-x)}O_{19}$, Solid-phase sintering, M-type strontium ferrite, Lattice constants.

INTRODUCTION

As a function of the electronics of the strontium ferrite material ($SrFe_{12}O_{19}$) a stable hexagonal magnetoplumbite type (M-type) structure, a high coercive force and energy product, the uniaxial magnetic anisotropy is in a microwave absorbent perpendicular magnetic recording material and high density magnetic materials have the potential of fine materials[1-5]. Currently available high-performance strontium ferrite calcined powders, research is focused on optimizing the preparation process and add some elements ions replace other considerations[6,7]. Performance using doped strontium ferrite magnet ($SrFe_{12}O_{19}$) currently has a large number of studies have reported[8,9], but the study report prepared by using yttrium (Y)-doped strontium ferrite has not yet appeared mixed use Miscellaneous strontium ferrite.

EXPERIMENTAL

Prepared by solid-phase sintering experimental samples[10,11]. According to the chemical structural formula $SrY_xFe_{(12-x)}O_{19}$ (x = 0, 0.25, 0.5, 0.75, 1) measurement, $SrCO_3$,Y_2O_3, Fe_2O_3 was prepared from experimental samples. Preparation process is as follows: **(1) Mixing:** Powders of $SrCO_3$,Y_2O_3,Fe_2O_3 were mixed with water, Ball by Material: Water: Ball mixing ratio = 1:1:8. Ball milling the ingredients of the above obtained mixture was stirred for 10 h to obtain an average particle size of suspended particles is 0.1-2 μm in mixture. **(2) Pre-Burn:** Mixture obtained in the preceding step and incubated at 1150 °C fired for 3 h to obtain a copper doped W-type strontium ferrite calcined material and then crushed to a coarse particle size of 0.8-1 μm Powder. **(3) Add two materials:** The material obtained above was calcined powders gluconate surfactant is added, then the mixed powder in a weight ratio of water: Material: Ball milled to an average particle = 1:1:8 diameter of 0.68 μm. **(4) Pressing the green body:** The orientation of the magnetic field of 15 KOe under a pressure at 0.5 ton/cm^2 pressed with a diameter of 20 mm, thickness of 6 mm green. **(5) Sintering:** The green body at 1260 °C, the air into the oxidizing atmosphere sintering temperature 3 h, cooled to room temperature after sintering GB/T3217-92 magnetic block for cutting and grinding national standards[12].

Using MACM-18XHF X-ray powder diffractometer (Cu target, Kα radiation, tube voltage 36 KV, tube current 20 mA, scanning speed of 4°/min) analysis of the powder phase composition, using JSM-7600F scanning electron microscope sample preparation The surface morphology analysis using

NIM-2000HF measuring magnetic properties of magnetic materials magnetic properties of the sample system for detection and analysis.

RESULTS AND DISCUSSION

The amount of yttirium dopant (x = 0,0.25, 0.5, 0.75, 1) at the calcination temperature for 3 h under 1295 °C prepared M-type strontium ferrite permanent magnet for X-ray diffraction (XRD) analysis. Fig. 1 shows the different strontium doping (x = 0,0.25, 0.5, 0.75, 1) of $SrY_xFe_{(12-x)}O_{19}$ (1295 °C sintering, 3 h) preparation obtained XRD patterns of permanent ferrite magnets. As can be seen from the figure, the samples have obvious W-type hexagonal ferrite phase (JCPDS 84-1531). Wherein the bottom lines of x = 0 XRD patterns of the $BaMg_2Fe_{16}O_{27}$ standard. Qualitative analysis by phase, $SrY_xFe_{(12-x)}O_{19}$ powder is γ-Fe_2O_3 principal phase and a very small amount of α-Fe_2O_3. When x respectively 0.25, 0.50, 1 the main phase is γ-Fe_2O_3 single phase, when x is 0.75, the main phase is γ-Fe_2O_3 phase and a small amount of α-Fe_2O_3 phase. XRD phase composition of the sample preparation and the W-type hexagonal ferrite phase characteristics typical match[13].

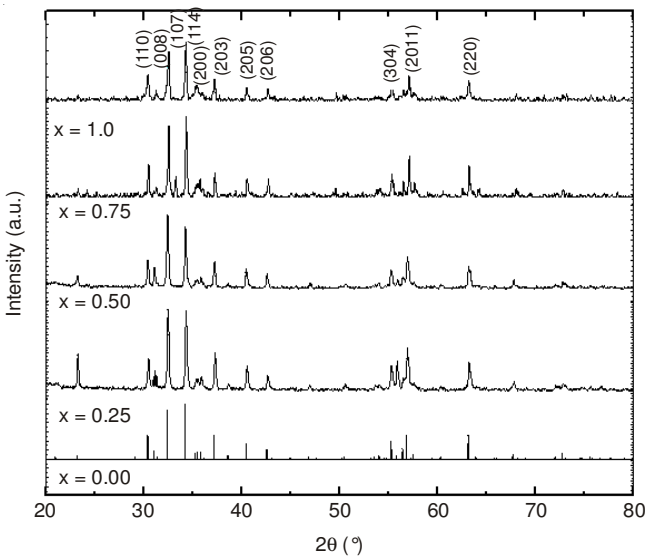

Fig. 1. XRD patterns of samples $SrY_xFe_{(12-x)}O_{19}$ sintered at 1295 °C for 3 h

$SrY_xFe_{(12-x)}O_{19}$ lattice constant of magnet: To the diffraction peak (008) and (107) of the hexagonal basis dhkl value calculated spacing of lattice constant a and c. Hexagonal strontium ferrite crystal structure, according to the hexagonal lattice spacing dhkl with lattice constants a and c, the relationship between[14]:

$$\frac{1}{d^2} = \frac{4}{3}\left(\frac{h^2 + hk + k^2}{a^2}\right) + \frac{l^2}{c^2} \quad (1)$$

wherein the Miller indices hk*l* (Miller Index), calculated for different doped yttrium $SrY_xFe_{(12-x)}O_{19}$ lattice constant a and c. And the crystal X-ray density $d_{x\text{-}ray}$ calculated by the following formula[15]:

$$d_{x-ray} = \frac{2M}{NAV_{cell}} \quad (2)$$

where M is the molecular weight of strontium ferrite doped Y, NA = 6.02 × 1023 is Avogadro (Avogadro) constant, V_{cell} = a2c/2 the volume of the hexagonal unit cell, factor " 2 " for the M-type hexagonal unit cell contained strontium ferrite number of molecules .

Table-1 shows the preparation of different doped yttrium $SrY_xFe_{(12-x)}O_{19}$ lattice constant a, c, a/c and the molecular weight, the crystal X-ray density values $d_{x\text{-}ray}$. As can be seen from Table-1, the lattice constant a with the substitution amount x increases yttrium rendered very small changes. Lattice constant c and the amount of yttrium substituted increase monotonically increasing x . Crystal X-ray $d_{x\text{-}ray}$ density increases approximately linearly. This is the lattice constant of a hexagonal ferrites showed essentially the same characteristics and changes in lattice constant c numerical characteristics often coincide[16]. Change in lattice constant may Y^{3+} (ionic radius 0.090 nm) instead of Fe^{3+} (ionic radius 0.067 nm), the larger the radius of Y^{3+} is difficult to replace the volume effects in magnetoplumbite structure hexagonal ferrite lattice sides $4f_1\uparrow$ body position Fe^{3+}, bound preferentially $2b\uparrow$ hexahedral position and $2a\uparrow$, $12k\uparrow$, $4f_2\downarrow$ octahedral sites. Ionic lattice distortion caused by changes in the radius increased, may also exist Y^{3+} (ionic radius 0.090 nm) instead of Fe^{3+} (ionic radius 0.067 nm) can change due to crystal binding factor, which explains both yttrium into the crystal lattice of strontium ferrite structure.

TABLE-1
LATTICE CONSTANTS, a/c AND FORMULA WEIGHT, X-RAY DENSITY FOR SAMPLES OF $SrY_xFe_{(12-x)}O_{19}$ (SINTERING TEMPERATURE IS 1295 °C, 3 h)

x	a (nm)	c (nm)	a/c	m.w. (g mol^{-1})	V_{cell} (10^{-18} cm^3)	$d_{x\text{-}ray}$
0	0.5861	2.3027	0.2545	1061.82	0.6850	5.15
0.25	0.5867	2.3032	0.2547	1070.09	0.6866	5.18
0.50	0.5871	2.3056	0.2546	1078.35	0.6882	5.21
0.75	0.5876	2.3105	0.2543	1082.62	0.6909	5.22
1.00	0.5869	2.3112	0.2539	1094.88	0.6894	5.28

Microstructure identification: $SrY_xFe_{(12-x)}O_{19}$ (1295 °C sintering, 3 h) isotropic ferrite magnet scanning electron micrograph (Fig. 2). $SrY_xFe_{(12-x)}O_{19}$ (1295 °C sintering, 3 h) anisotropic ferrite magnet along the C axis parallel to the direction of scanning electron micrographs (Fig. 3). $SrY_xFe_{(12-x)}O_{19}$ (1295 °C sintering, 3 h) anisotropic ferrite magnet along the C-axis perpendicular to the direction of scanning electron micrographs (Fig. 4). The permanent ferrite magnets in the C-axis perpendicular to the direction of the typical hexagonal morphology, the C-axis parallel to the direction of the rectangular obvious characteristics, the prepared hexagonal ferrite material is characterized by crystal lattice the typical morphology[17].

Magnetization: Fig. 5 is 1295 °C sintered for 3 h, yttrium doping for x = 0.5 $SrY_xFe_{(12-x)}O_{19}$ prepared strontium ferrite permanent magnet demagnetization curve, respectively Table-2 lists $SrY_xFe_{(12-x)}O_{19}$ (x = 0, 0.25, 0.5, 0.75, 1) preparation of strontium ferrite magnets remanence B_r, coercive force magnetic induction H_{cb}, H_{cj} intrinsic coercivity and maximum energy product (BH) max. As can be seen from the table, when Y doping amount is increased, $SrY_xFe_{(12-x)}O_{19}$ with remanence B_r increases monotonically with $SrY_xFe_{(12-x)}O_{19}$ compared

TABLE-2
REMANENCE B_r, MAGNETIC COERCIVITY H_{cb}, INTRINSIC COERCIVITY H_{ci} AND MAXIMUM ENERGY PRODUCT $(BH)_{max}$ OF $SrY_xFe_{(12-x)}O_{19}$ (x= 0, 0.25, 0.5, 0.75, 1.0) (SINTERED AT 1295 °C FOR 3 h) PERMANENT MAGNET, RESPECTIVELY

x	B_r (mT)	H_{cb} KA m^{-1})	H_{cj} (KA m^{-1})	$(BH)_m$ (KJ m^{-3})
0	384.7	265	286.7	28.9
0.25	400.5	287.2	312.3	31.9
0.5	409.5	305.4	329.7	33
0.75	410.4	306.7	323.7	33.1
1	420.7	256.5	276.6	32.6

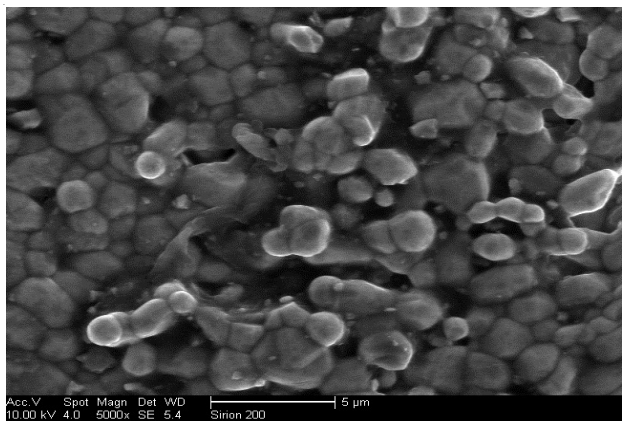

Fig. 2. SEM patterns of samples of isotropic ferrite prepared by $SrY_xFe_{(12-x)}O_{19}$ (sintered at 1295 °C for 3 h)

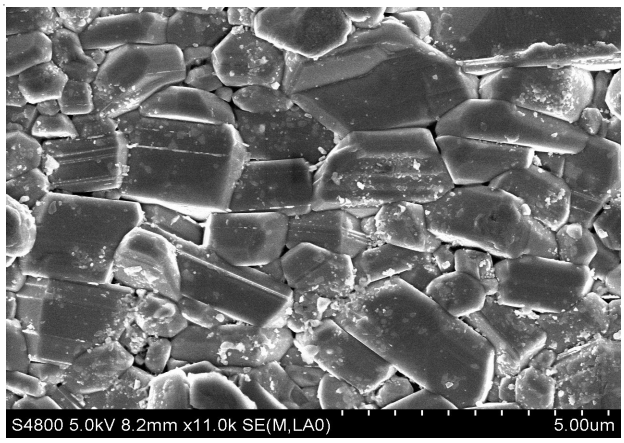

Fig. 3. SEM patterns of samples along the C axis parallel orientation of anisotropy ferrite prepared by $SrY_xFe_{(12-x)}O_{19}$ (sintered at 1295 °C for 3 h)

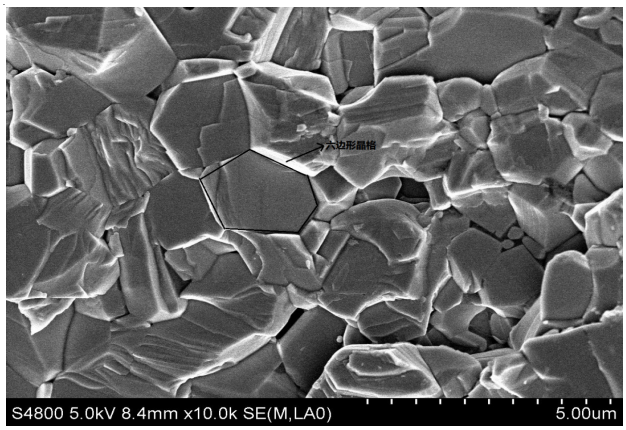

Fig. 4. SEM patterns of samples along the C axis perpendicular orientation of anisotropy ferrite prepared by $SrY_xFe_{(12-x)}O_{19}$ (sintered at 1295 °C for 3 h)

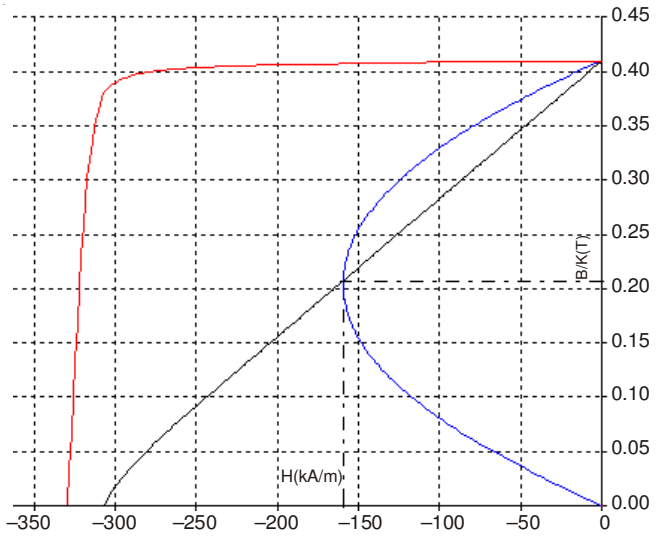

Fig. 5. Demagnetization curve of $SrY_{0.5}Fe_{11.5}O_{19}$ (sintered at 1295 °C for 3 h) permanent magnet

remanence B_r, enhance the rate of nearly 10 %. This may be due Y^{3+} replaces Fe^{3+} caused a significant change in remanence B_r. H_{cj} intrinsic coercivity first increases and then decreases when x = 0.75 when H_{cj} reached the maximum 323.7 KA m^{-1}, while the remanence B_r reached 410.4 mT. Coercivity magnetic induction H_{cb} H_{cj} trends and variation of the same, first increases and then decreases. Maximum energy product [(BH) max] first increases and then decreases. When x = 1, the maximum remanence B_r, but the intrinsic coercivity H_{cj} goes in the minimum, which is strontium ferrite magnet of remanence B_r and intrinsic coercivity of mutual restraint between H_{cj} the relationship pertinence[18]. Therefore, the amount of yttrium-doped strontium ferrite magnet help to improve the comprehensive magnetic properties; yttrium doping at x = 0.75 when approaching suitable for preparing high intrinsic coercivity of strontium ferrite; yttrium doping in close x = 1 is suitable for preparing high remanence strontium ferrite.

Conclusion

Solid-phase reaction method yttrium-doped strontium ferrite process is simple and reasonable. When using solid-phase sintering at 1150 °C heat sintering for 3 h preparing the yttrium-doped M-type strontium ferrite $SrY_xFe_{(12-x)}O_{19}$ (x = 0, 0.25, 0.5, 0.75, 1) calcined material and then the pre- use orientation of the magnetic field burning materials after pressing for 3 h under 1295 °C sintered magnets. Prepared $SrY_xFe_{(12-x)}O_{19}$ (1295 °C sintering, 3 h) with complete magnetoplumbite type hexagonal structure, the main phase is substantially a single γ-Fe_2O_3.

As Y-doped increases, the lattice constant a substitution amount x increases as the display very small changes; lattice constant c as the substitution of yttrium increases monotonically with increase of x; crystal X-ray density $d_{x\text{-ray}}$ approximately linearly increases.

With the Y doping increases, $SrY_xFe_{(12-x)}O_{19}$ remanence B_r increases monotonically with; H_{cj} intrinsic coercivity first increases and then decreases when x = 0.75 at maximum H_{cj} value 323.7 KA m^{-1}, while the remanence B_r reached 410.4 mT; coercivity magnetic sense H_{cb} first increases and then

decreases; maximum energy product (BH) max first increases and then decreases. When x = 1, the maximum remanence B_r, but the intrinsic coercivity H_{cj} subsequently becomes minimum.

On the Y-doping close to x = 0.75 is suitable for the preparation of high intrinsic coercivity of strontium ferrite; close to the Y-doping when x = 1 suitable for preparing high remanence strontium ferrite.

ACKNOWLEDGEMENTS

This work was supported in part by Science Foundation of Suzhou University under Grant No. 2013YKF26 and by master fund of Suzhou University under Grant No. 2009YSS08.

REFERENCES

1. Y.S. Hong, C.M. Ho, H.Y. Hsu and C.T. Liu, *J. Magn. Magn. Mater*., **279**, 401 (2004).
2. A. Mali and A. Ataie, *Scr. Mater*., **53**, 1065 (2005).
3. A. Vijayalakshmi and N.S. Gajbhiye, *J. Appl. Phys*., **83**, 400 (1998).
4. S.A. Oliver, S.D. Yoon, I. Kozulin, M.L. Chen and C. Vittoria, *Appl. Phys. Lett*., **76**, 3612 (2000).
5. N. Kishan Reddy and V.N. Mulay, *Mater. Chem. Phys*., **76**, 75 (2002).
6. Z. Pang, X. Zhang, B. Ding, D. Bao and B. Han, *J. Alloys Comp*., **492**, 691 (2010).
7. N. Chen, K. Yang and M. Gu, *J. Alloys Comp*., **490**, 609 (2010).
8. P. Sharma, A. Verma, R.K. Sidhu and O.P. Pandey, *J. Alloys Comp*., 361, 257 (2003).
9. G. Litsardakis, I. Manolakis and K. Efthimiadis, *J. Alloys Comp*., **427**, 194 (2007).
10. X.R. Tang, Central South University Press, pp. 174-184 (1992).
11. J. Fu, T. Jiang and D. Zhu, Central South University Press, pp. 125-151 (1996).
12. X.S. Liu, D. Zhu and P. Yin, A Calcium Ferrite Material and Method, 200910251673.3.
13. X.S. Liu, D.N. Jia, F. Hu, *et al*.., *Rare Metal Mater. Des*., **9**, 63 (2012).
14. T.J. Chang and X. Qi, Harbin Institute of Technology Press, Heilongjiang, China, pp. 64-76 (1999).
15. G. Xu, H. Ma, M. Zhong, J. Zhou, Y. Yue and Z. He, *J. Magn. Magn. Mater*., **301**, 383 (2006).
16. R.P. Cowburn and M.E. Welland, *Science*, **287**, 1466 (2000).
17. P. Berthet, J. Berthon, G. Heger and A. Revcolevschi, *Mater. Res. Bull*., **8**, 919 (1992).
18. R.C. Pullar, *Prog. Mater. Sci.*, **57**, 1191 (2012).